Journal of the Korea Concrete Institute
Vol.16 No.2, pp.277~282, April, 2004

Pore Size Distribution and Chloride Diffusivity of Concrete Containing Ground Granulated Blast Furnace Slag

Han-Young Moon[1)*], Hong-Sam Kim[2)], and Doo-Sun Choi[1)]

[1)] *Dept. of Civil Engineering, Hanyang University, Seoul, Korea*
[2)] *Dept. of Civil Engineering, Daejin University, Korea*

(Received December 26, 2003; Accepted March 30, 2004)

Abstract

In a hardened concrete, diffusion of oxygen, carbon dioxide, aggressive ions, and moisture from the environment to the concrete takes place through the pore network. It is well known that making dense cement matrix enhances the durability of concrete as well as all the characteristics including strength of concrete.

In this paper, 9 mix concretes with water to cementitious material ratio (40, 45, and 50%) and replacement ratio of GGBFS (40 and 60% of cement by weight) were studied on the micro-pore structure by mercury intrusion porosimetry and the accelerated chloride diffusion test by potential difference. From the results the average pore diameter and accelerated chloride diffusivity of concrete were ordered NPC > G4C > G6C. It is concluded that there is a good correlation between the average pore diameter and the chloride diffusivity, and the mineral admixtures has a filling effect, which increases the tortuosity of pore and makes large pores finer, on the pore structure of cement matrix due to the latent hydraulic reaction with hydrates of cement.

Keywords: mercury intrusion porosimetry, capillary pore, average pore diameter, chloride diffusivit

1. Introduction

Concrete is inherently a durable material. If concrete is properly designed and produced for the environment to which it will be exposed, the concrete is capable of maintenance-free performance for decades without any need for protective management, except highly corrosive environments. Concrete, however, is potentially vulnerable to a variety of exposures unless certain precautions are taken.

The deterioration factors of concrete are freezing and thawing, alkali-aggregate reaction, carbonation, chemical attack, and steel corrosion by penetration and diffusion of chloride ion.[1,2)]

It was well known that most chemical and physical processes that degrade cementitious materials are dependent on an external source of either water or ions or the both. Corrosion of steel bars in reinforced concrete, for example, depends on the chloride concentration at the bar, which needs to reach a critical level for the initiation of corrosion.

* *Corresponding author*
Tel.: +82-2-2290-0323 Fax : +82-2-2293-9977
E-mail address: moon77@hanyang.ac.kr

Chloride ions from external sources can only reach the bars through water-filled pore space. Sulfate attack is dependent on sulfate ion transport through the water-filled pores. The movement of water in the pore-void essentially determines the freezing and thawing resistance. In order to develop a sound scientific basis for prediction and control of service life of a cement-based material, therefore, it is necessary to understand the mechanisms of these processes at the micro-structural level. An important step in developing this knowledge is to understand how rates of transport, characterized by values of transport coefficients such as diffusivity and permeability, depend on the details of the porous microstructure.

On the other hand, the pore of porous media is generally divided to micro-, meso-, and macro-pore by pore size, and that of cement matrix is divided to gel, capillary, ITZ (interfacial transition zone) pore, and air content.

Many researchers studied the size of gel and capillary pore, but the classification of pore size in cement matrix is different from each other. For example, Metha demonstrated that the pore of cement matrix is largely gel- (<5nm)

Table 1 Oxides composition and physical properties of cement and mineral admixture

Types \ Items	Chemical compositions (%)						Physical properties	
	SiO_2	Al_2O_3	Fe_2O_3	CaO	MgO	SO_3	Specific gravity	Blaine(cm^2/g)
NPC	19.88	4.81	3.11	61.56	2.95	2.82	3.15	3,120
GGBS	31.88	12.64	0.39	42.46	6.38	3.63	2.92	4,450

and capillary-pore (5~100nm), again, the latter is divided to micro-pore (5~50nm) affecting the dry shrinkage and creep of cement matrix and macro-pore (50~100nm) on the strength and ion penetration.[2)]

In addition, the pore structure of cement matrix change with cement type, admixtures, degree of hydration, and concrete mixing.[3,4)] In this paper, 9 mix concretes using normal Portland cements and 2 types of blended cements were studied on the micro-pore structure by mercury intrusion porosimetry and accelerated chloride diffusion test by potential difference. The test results show that there is a good correlation between the average pore diameter and the chloride diffusivity of concretes.

2. Experiments

2.1 Materials

Normal Portland cement (NPC) specified in KS L 5201 and blended cement (G4C and G6C) with ground granulated blast-furnace slag (GGBFS) were used in all concrete mixtures. GGBFS was used to replace cement at ratio of 40 and 60% by weight. The oxides analysis and physical properties of the materials employed in the experimental program are presented in Table 1.

Table 2 Physical properties of aggregates

Agg. \ Items	G_{max} (mm)	Specific gravity	Absorption (%)	F.M.
Fine	-	2.58	0.80	2.65
Coarse	25	2.62	0.78	6.83

River sand, which is immune to most chemical agents and has little organic compounds, and crushed stone were employed for manufacturing concrete specimens. The specific gravities of fine and coarse aggregates are 2.58 and 2.62, respectively. Physical properties of the aggregate are listed in Table 2.

Concrete specimens were prepared as $\phi 100 \times 200$mm cylinders, demoulded at 24-hour after casting and then cured for 28 days in water (at 23℃).

Concrete mixtures with water to cementitious material ratio (W/cm) of 40, 45, and 50% used in this study are listed in Table 3. Compressive strength test at 28-day (denoted f_{28}) was conducted and presented in Table 3.

AE water reducing agent with specific gravity 1.09 was additionally applied to obtain target air content and reduce unit water.

2.2 Micro-structural analysis

BET, MIP, and X-ray CT were conventional methods for measuring the pore size distribution in a porous media.

Of these methods, mercury intrusion porosimetry is a widely used method for measuring the pore size distribution of cement matrix. It is based on the fact that for squeezing out a non-wetting fluid in a pore of the diameter d, a pressure P inversely proportional to the diameter of this pore must be applied.

For a cylindrical pore, pore diameter (d) is determined by the Washburn Eq. (1).

Table 3 Mix proportions of concrete

Types \ Items	W/cm (%)	S/a (%)	Unit weight (kg/m^3)					Slump (cm)	Comp. strength f_{28} (Mpa)
			W	C	S	G	GGBS		
NPC	40	41	187	468	655	957	-	13	44.2
	45	42	187	416	689	967	-	14	37.8
	50	43	187	374	720	970	-	14	34.6
G4C	40	41	187	281	650	951	187	15	45.5
	45	42	187	249	685	960	166	15	41.7
	50	43	187	224	716	964	150	15	36.2
G6C	40	41	187	187	648	947	281	15	44.7
	45	42	187	166	683	957	249	15	38.8
	50	43	187	150	714	961	224	16	35.5

$$d = \frac{-4 \cdot \gamma \cdot \cos\theta}{P} \quad (1)$$

Where, γ is the surface energy of the liquid, θ is the contact angle (130°). And, the average pore diameter of capillary pore (D_a) is given as seen in Eq. (2).

$$D_a = \frac{4V_t}{S_t} \quad (2)$$

where, V_t and S_t is the total pore volume and total surface area of capillary pore respectively.

The fraction of porosity occupied by pores with diameters in the interval (d; $d+\delta d$) is then deduced from the volume of mercury intruded in the pressure range (P; $P+\delta P$), supposing that all the pores are directly connected to the source of mercury. As this hypothesis is not generally verified, it turns out that the measured and the real pore size distributions differ significantly. Thus, capillary pore in this paper was confined to 0.003~10 μm as the range of confidence in MIP test.

The concrete specimens at 28-day were crushed and mortar portion were obtained. The pieces weighed about 1.5g and were kept in a dry oven at 105~110℃ for 24 hours. Then, the MIP test was conducted.

2.3 Determination of chloride diffusivity

The conventional diffusion cell method was used to determine the diffusivity of the corresponding portions of the specimens. Since the diffusion cell test would take months, the accelerated test by potential difference was conducted in this study.

The central portion of specimens was cut into 50mm thick slices after 28 days of curing, the other procedures of the accelerated chloride diffusion test is similar to those proposed by Tang et. al. and Moon et. al.[5,6]

Experimental conditions in this test are listed in Table 4. The accelerated chloride diffusivity of concrete was determined by Eq. (3).[5-7]

$$D_{acc} = \frac{RTL}{zFU} \cdot \frac{x_d - \alpha\sqrt{x_d}}{t} \quad (3)$$

where, $\alpha = 2\sqrt{\frac{RTL}{zFU}} \cdot erf^{-1}\left[1 - 2\frac{C_d}{C_o}\right]$

D_{acc}: accelerated chloride diffusivity (m^2/s)
R: gas constant, F: Faraday's constant
T: absolute temperature (K), z: balance ion
L: thickness of specimen (m), t: testing time (sec.)
U: potential difference (V)
X_d: penetration depth by colorimetric method

Table 4 Experiment conditions for accelerated test

Thickness (mm)		50
Electrolyte solutions	Cell I (-)	0.5M NaCl
	Cell II (+)	Sat. $Ca(OH)_2$
Testing time (hr.)		8
Measurement factor		Penetration depth

C_0: concentration of Cl^- in cathode cell (mol/l)
C: reaction concentration by colorimetric method
A: experimental constant (α=23,600m^{-1})
erf: error function

To find the relationship between pore structure and chloride diffusivity of concrete at the same ages, electrical accelerated test, which is commonly used to estimate the diffusion coefficient of chloride ions, was applied. Therefore, estimated diffusion coefficient in this study is different from the diffusion coefficient by concentration difference at steady state or immersion test.

3. Results and discussion

3.1 Pore size distribution of concretes

Although MIP involves a number of experimental complications, its principle is basically simple. In the present study, in order to understand more easily the pore structure of hardened cement matrix, MIP was conducted on 9 mix concretes with W/cm of 40, 45, and 50%.

As shown in Fig. 1, the pore size of porous media is divided into micro-pore for <0.01 μm, meso-pore for 0.01~0.05 μm, and macro-pore for 0.05~10 μm, while the pore of cement matrix is divided into gel-pore for <0.003 μm,

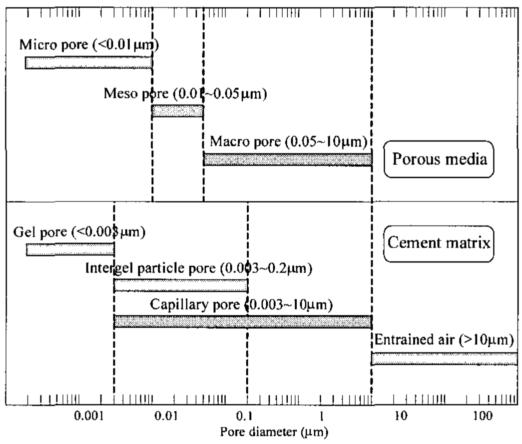

Fig. 1 Classification of pore size

inter-particle pore for 0.03~200 μm, capillary-pore for 0.003~10 μm, and entraining air void for > 10 μm to analyze the pore structure of concrete.[6] Fig. 2 presents the pore size distribution of 9 mix concretes. The major peak of NPC was meso-pore about 0.03 μm, whereas that of G4C and G6C were micro-pore about 0.006~0.008 μm.

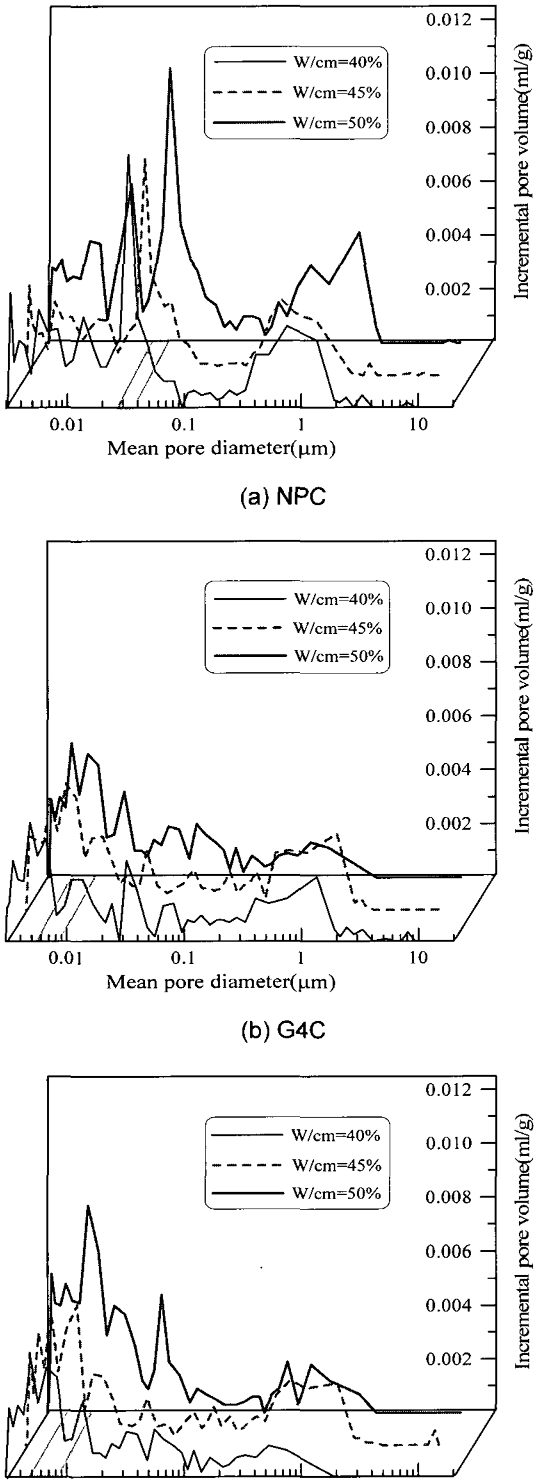

(a) NPC

(b) G4C

(c) G6C

Fig. 2 Pore size distribution of concretes

The detailed data of MIP are presented in Table 5. The average pore diameter of blended cement was less than that of Portland cement. The difference of average pore diameter between NPC and GGBS concretes appears to be because mineral admixture makes the inter-particle pore of concrete denser. In the case of the cumulative pore volume, as shown in Fig. 3, GGBS concretes have the different shape regardless of W/cm around 0.05 μm compare to NPC concretes. GGBS concretes, that is, have the denser pore structures than that of NPC concretes. Thus, GGBS improves the corrosion protection and strength of the concrete by reducing the porosity of concrete. It appears to result that GGBS activated by $Ca(OH)_2$ formed during hydration form a mixture of C-S-H, C-A-H, and AF_m phases.[8] In addition to this, tiny particles of the GGBS may help distributing of the particle and the packing of the system, and leading to lower permeability of the concrete.

3.2 Chloride diffusivity of concretes

It is well known that the durability of concrete is significantly affected by the permeation of aggressive ions migrated into the hardened cement matrix. The accelerated chloride diffusion test by potential difference was used to estimate the chloride diffusivity of concrete.

Fig. 4 shows the accelerated chloride diffusivity of NPC, G4C, and G6C concretes at 28 days. From Fig. 4, it appears that NPC concretes exhibit a larger diffusion coefficient compared with GGBFS concretes, and the order of chloride diffusivity regardless of W/cm was ordered NPC > G4C > G6C. That is, chloride diffusivity for GGBFS concretes was the level of 40~60% compared with that of NPC concrete.

This may be due to the filling effect and the latent hydraulic reaction of GGBFS. The addition of mineral admixtures into cement can modify the microstructure of cement matrix by forming more C-S-H gel from latent hydraulic reactions and by filling the pores with their fine particles.[9]

Thus, low permeability of cement matrix with mineral admixtures limits the penetration of aggressive ions such as chloride ion, sulfate, and carbon dioxide.

Besides, to investigate the hydrated texture of cement matrix, its micro-structures were examined using FE-SEM at the same magnification.

Table 5 Pore analysis results of concrete (0.003~10 μm, 28 days)

Types \ Items	Average pore diameter (μm)		
	W/cm=40%	W/cm=45%	W/cm=50%
NPC	0.0115	0.0125	0.0121
G4C	0.0097	0.0097	0.0083
G6C	0.0088	0.0090	0.0075

Fig. 5 shows FE-SEM images for mortar portion of concretes with W/cm=40% at 90 days.

As can be the Fig. 5, the pore structures of NPC FE-SEM image (Fig. 5(a)) is loose, whereas that of GGBFS concretes (Fig. 5(b), (c)) denser. The fineness of hydrated structure of concretes increased with increasing the replacement ratio of GGBFS.

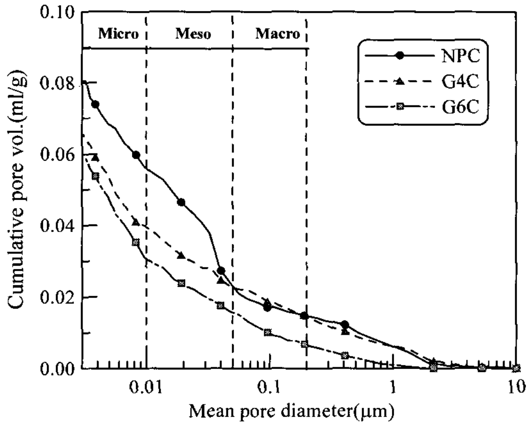

(a) W/cm = 40%

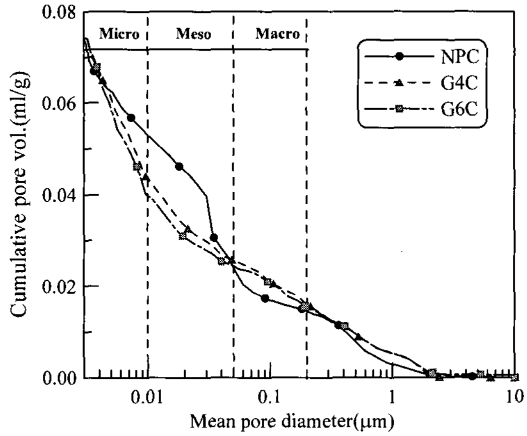

(b) W/cm = 45%

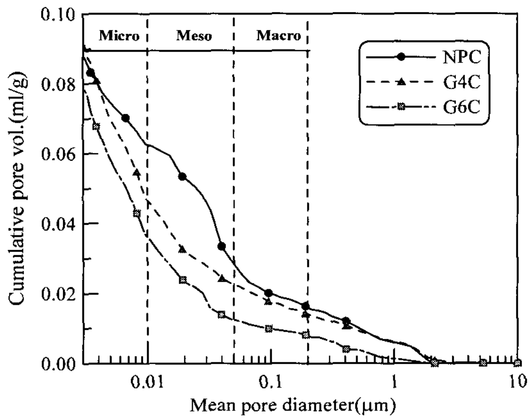

(c) W/cm=50%

Fig. 3 Distribution of cumulative pore volume

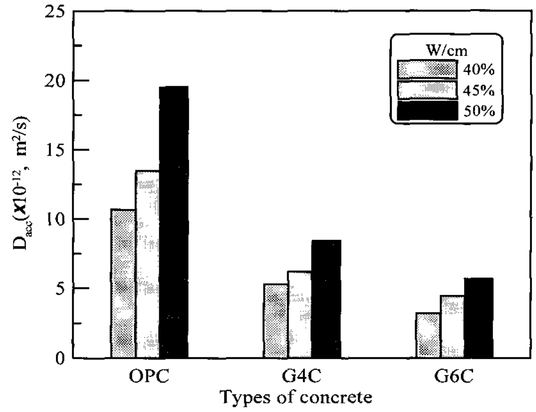

Fig. 4 Chloride diffusivity by accelerating test

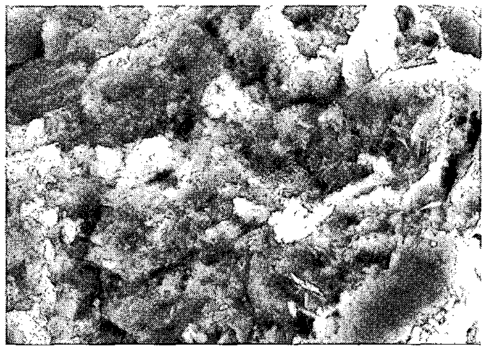

(a) Image of NPC

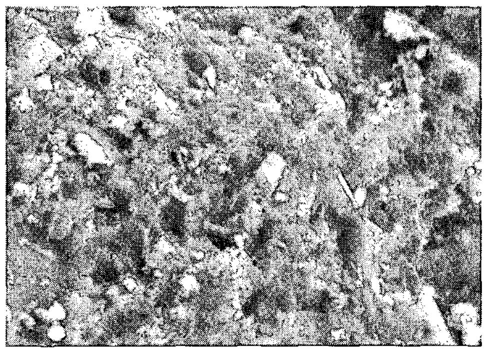

(a) Image of G4C

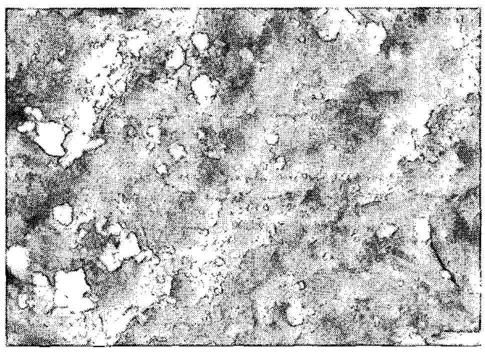

(c) Image of G6C

Fig. 5 SEM Images of cement matrices

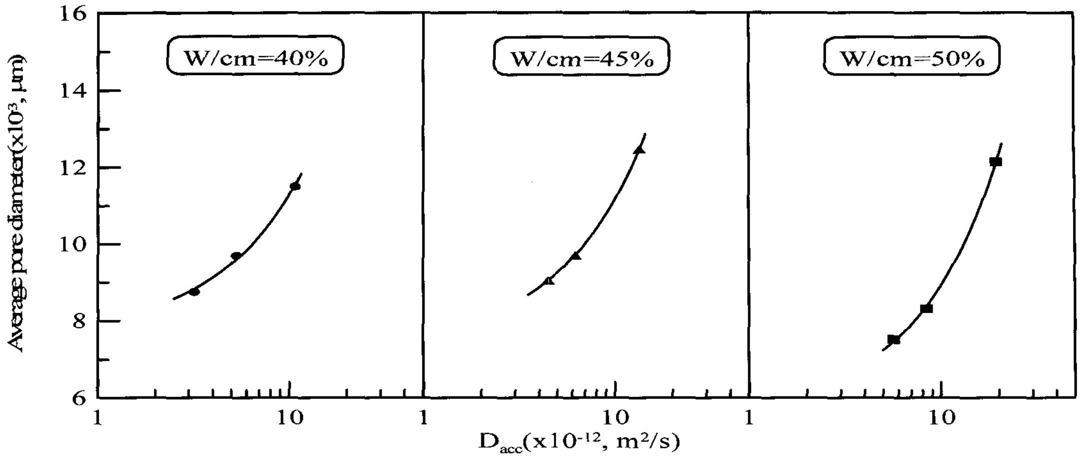

Fig. 6 Relationship between chloride diffusivity and average pore diameter with W/cm

3.3 Average pore diameter and chloride diffusivity

To know the correlation between the accelerated chloride diffusivity and the characteristic of pore structure of concrete, the relationship between the accelerated chloride diffusivity and average pore diameter of concrete with W/cm=40, 45, and 50% was analyzed. The result is presented in Fig. 6. From this figure, it seems that there is a good correlation between the average pore diameter and the chloride diffusivity. Thus, we conclude the following;

1) The penetration property of chloride ion in concrete and the pore size distribution of concrete have a close relationship. Especially when using the mineral admixtures, a number of pores more than 0.05 μm in concrete decreases.
2) The factor affecting chloride diffusivity of concrete is not the total pore volume of concrete but the average pore diameter of concrete.

4. Conclusion

The conclusion of this paper is as follows;

1) The peak of incremental pore volume was around about 0.03 μm for Portland cement, and 0.006~0.007 μm for blended cement regardless of W/cm. Also, the cumulative pore volume of concrete increased with increasing W/cm.
2) Average pore diameter of capillary pore was ordered NPC > S4C > S6C. Average pore diameter for Portland cement was above 0.01 μm, while was beneath 0.01 μm for blended cement.
3) Accelerated diffusivity of chloride ion regardless of W/cm was ordered NPC > S4C > S6C. The formation of dense pore structure due to mineral admixtures leads to decrease in average pore diameter and chloride diffusivity of concrete.
4) There was a good correlation between the average pore diameter and the chloride diffusivity, and the mineral admixtures has a filling effect on the pore structure of cement matrix due to the latent hydraulic reaction with hydrates of cement, which increases the tortuosity of pore and makes large pores finer.

Reference

1. Haque M. N. and Kawamura M., "Carbonation and Chloride-Induced Corrosion of reinforcement in Fly Ash Concrete," *ACI Materials Journal*, Vol.89, No.1, 1992, pp.44~48.
2. Metha P. K., Monterio R. K., "*Concrete-Structure, Properties, and Materials*," Prentice Hall, New Jersey, 1993, pp.167 ~168.
3. Torii K., Miyoshi M., and Masuda T., "Electrical Resistivity and Coefficient of Chloride Diffusion of Portland Cement-Fly Ash Paste," *Proceedings of the Japan Concrete Institute*, Vol.18, No.1, 1996, pp.951~956.
4. Jones M. R., Dhir R. K., and Magee B. J., "Concrete Containing Ternary Blended Binders: Resistance to Chloride Ingress and Carbonation," *Cement and Concrete Research*, Vol.27, 1997, pp.825~831.
5. Tang L. and Nilsson L.O., "Rapid Determination of the Chloride Diffusivity in Concrete by Applying an Electrical Field," *ACI Materials Journal*, Vol.89, No.1, 1992, pp.49~53.
6. Han-Young Moon, Hong-Sam Kim, and Doo-Sun Choi, "The Characteristic of Capillary Pore and Chloride Diffusivity by Electrical Difference into Various Concrete," *Journal of the Korean Society of Civil Engineers*, Vol.23, No.5A, 2003, pp.969~976.
7. Tang L. O., "Electrically Accelerated Methods for Determining Chloride Diffusivity in Concrete –Current Development," *Magazine of Concrete Research*, Vol.48, No.176, 1996, pp.173~179.
8. Sidney Mindess, J. Francis Young, and David Darwin, "*Concrete*," Prentice Hall, 2nd Edition, New Jersey, 2003, pp.102~104.
9. Shiqun L. and Roy D. M., "Investigation of Relations between Porosity, Pore Structure and Cl- Diffusion of Fly Ash and Blended Cement Paste," *Cement and Concrete Research* Vol.16, No.5, 1986, pp.749~759.